RSC Advances

PAPER

An imidazopyrazine-derived anion for lithium conducting electrolyte application

Leszek Niedzicki,* Jędrzej Korczak, Anna Bitner, Maria Bukowska and Przemyslaw Szczecinski

Cite this: *RSC Adv.*, 2015, **5**, 101917

Received 7th August 2015
Accepted 10th November 2015

DOI: 10.1039/c5ra15869a

www.rsc.org/advances

In this work we present a new lithium salt of 4,5-dicyano-2-(trifluoromethyl)imidazopyrazine (LiTDPI) which was designed for use as an electrolyte in lithium-ion cells. It was synthesized and completely characterized by NMR techniques. The salt is thermally stable up to 350 °C and electrochemically stable in carbonate solvents up to +5.1 V *vs.* Li. Basic electrochemical characterization of this new lithium salt solution shows conductivity of over 2 mS cm^{-1} at room temperature and a transference number which is higher than the commercial reference salt, $LiPF_6$ (>0.4 in a EC : DMC 1 : 2 ratio mixture). As a proof of concept, short cycling measurements in a graphite half-cell show good capacity (352 mA h g^{-1}) and capacity retention (96% after 50 cycles). The extremely good stability without compromising the performance parameters shows the next leap in progress for tailoring efficient lithium-conducting electrolytes.

1. Introduction

For the last 20 years lithium batteries have been the fastest growing technology and are now established as the battery of choice in the energy storage market.[1] Emerging areas, but soon-to-be mass applications, of energy storage like electric vehicles and grid storage are focusing mainly on lithium-ion technology. All modern mobile devices, mobile phones and notebooks are reliant solely on this technology as their energy source. Lithium-ion cells would not have their place on the market if not for the constant advance in their technology, *i.e.* the development of component materials engineering and chemistry. However, while there are plenty of scientific contributions on electrode material structure and manufacture, there is a huge gap in the electrolytic materials for this type of cell. Apart from $LiPF_6$, no other salt has been used in the wide scale production of commercial lithium-ion cells for the last 20 years. Although a lot of work and research on electrolytes is done every year, most work is based on two or three salts only, even though the salt influences most important cell parameters. For instance, its stability limits the maximum cell voltage, its conductivity influences the maximum safe current density in constant discharge and its lithium cation transference number influences the charge–discharge cycle efficiency.[2]

Despite the use of only two-three most popular salts among researchers, even the most popular ones, along with $LiPF_6$, have numerous disadvantages. To enumerate only the most important disadvantages: $LiPF_6$ is susceptible to hydrolysis, forming caustic HF and toxic POF_3 (ref. 3 and 4) and has poor thermal stability;[5] $LiClO_4$ is potentially explosive in high temperatures;[6] $LiAsF_6$ is toxic (as it contains arsenic); $LiCF_3SO_3$ (LiTf) conducts poorly;[7] $LiN(SO_2CF_3)_2$ (LiTFSI) and $LiN(SO_2C_2F_5)_2$ (LiBETI) corrode aluminum current collectors;[8] $LiPF_3(C_2F_5)_3$ (LIFAP) is too expensive during production;[4] and $LiB(C_2O_4)_2$ (LiBOB) forms a high-resistance SEI at high concentrations.[9] Thus, there is still a need for new concepts in the field of lithium salts for lithium-conducting electrolytes. Inspired by the success of lithium 4,5-dicyano-2-(trifluoromethyl)imidazolide (LiTDI)[10–12] we decided to follow the path of anion design towards another "tailored" anion for potential lithium-ion cell application.

Following our previous work on lithium 5,6-dicyano-2-(trifluoromethyl)benzimidazolide (LiTDBI),[13] in this paper we propose a new anion structure. Our new concept is based on LiTDBI, a benzene-derived anion, which has been previously modeled by Scheers *et al.*,[14] and tested by our group in electrolytes. The electrochemical parameters of the LiTDBI solution pass the minimal requirements for the cell electrolyte:[15] its conductivity is over 1 mS cm^{-1} at room temperature, the lithium cation transference number is over 0.3 (in fact it is *ca.* 0.5), it is soluble in organic carbonates, compatible with a graphite anode, has an electrochemical stability of over 4 V *vs.* Li (in fact over 4.6 V *vs.* Li) and a thermal stability of over 100 °C (in fact over 280 °C). Despite that, it has not defeated the parameters set by the state of the art salt, $LiPF_6$. That may stem from the hydrogen presence in the LiTDBI salt structure. Although the only hydrogens in the molecule are bonded to the aromatic carbons, they can still have their share of intermolecular interactions thanks to the possibility of hydrogen bonds forming with the solvent molecules. Thus, in this paper we show an enhancement of the LiTDBI structure made through

Warsaw University of Technology, Faculty of Chemistry, Department of Inorganic Chemistry and Solid State Technology, Noakowskiego 3, 00664 Warsaw, Poland. E-mail: lniedzicki@ch.pw.edu.pl; Fax: +48 22 628 2741; Tel: +48 22 234 7421

the removal of hydrogen atoms from the anion. This was performed by substituting the carbon atoms in the aromatic ring with nitrogen atoms. In this way we omitted unnecessary steric obstacles and possible proton sources, as well as the occurrence of the potential hydrogen bonds, for the small cost of having slightly higher polarization of the ring inner bonds. As a result we obtained the lithium salt of 4,5-dicyano-2-(trifluoromethyl) imidazopyrazine (which we have abbreviated to LiTDPI).

In this paper basic properties of the salt are reported. Apart from standard spectroscopic characterization, we also investigated the salt properties which influence the electrolyte parameters, such as stability. The basic electrochemical parameters of this new salt solution were also tested. Finally, only as a proof of concept, we also cycled the newly obtained electrolyte in a half-cell to check its potential for further development and optimization.

2. Experimental

2.1. Experimental techniques

Nuclear magnetic resonance (NMR) spectra were recorded on a Varian Gemini 500. The samples for NMR experiments were dissolved in deuterated dimethyl sulfoxide (DMSO-d_6, 99.96 atom% D, Aldrich). The ^{1}H and ^{13}C chemical shifts are reported relative to DMSO-d_6.

Thermogravimetric Analysis (TGA) was carried out on a Q50 thermogravimetric analyzer, TA Instruments. The carrier gas was argon and the heating rate was equal to 10 K min^{-1}.

All the samples used for measurement were assembled in an argon-filled drybox with a moisture level below 1 ppm. Prior to the assembly, the salt was vacuum-dried for 48 hours at 120 °C. The solvents—propylene carbonate (PC), ethylene carbonate (EC) and dimethyl carbonate (DMC)—were anhydrous and used as provided by Sigma-Aldrich (water content <20 ppm for PC and DMC, <50 ppm for EC).

Linear sweep voltammetry (LSV), cyclic voltammetry (CV), transference number, ionic conductivity and half-cell cycling measurements were carried out on a VMP3 multichannel potentiostat (Bio-Logic Science Instruments) with the frequency response analyzer option. All electrochemical experiments except for the conductivity measurements were performed at ambient temperature.

LSV and CV experiments were realized with the custom-made three electrode Swagelok-type cell, where the reference and counter electrodes were in the form of discs and the working electrode was a wire. The electrodes and separators soaked with electrolyte were sandwiched between the stainless steel punches. The platinum working electrode was a platinum wire put between separators from the side tight access port.

In the case of the LSV measurements, these were carried out in a three-electrode Li|electrolyte|Pt system (with lithium metal as the reference electrode). The LSV scan rate was 10 mV s^{-1}.

In the case of the CV measurements, these were carried out in the same cell as LSV and used a three-electrode Li|electrolyte|Al system (with lithium metal as the reference electrode). The CV scan rate was 0.1 mV s^{-1}.

For the ionic conductivity measurements electrochemical impedance spectroscopy (EIS) was employed and the samples were thermostated in a Haake D50 cryostat where the temperature was varied from −20 °C to 40 °C in 10 °C increments (with a precision of 0.05 °C), allowing an hour for stabilization.

The lithium cation transference number was determined using the standard Bruce–Vincent–Evans method[16] and the following equation: $T_+ = (I_s(\Delta V - I_0R_0))/(I_0(\Delta V - I_sR_s))$, where ΔV is the polarization voltage equal to 20 mV; I_0 and I_s are the initial and the steady-state current during said polarization, respectively; R_0 and R_s are the resistances of the solid electrolyte interface (SEI) immediately before and after the polarization, respectively. The Li|electrolyte|Li cells were used for the transference number experiments. The electrochemical impedance spectroscopy (EIS) used to obtain R_0 and R_s was performed with 5 mV amplitude over the 500 kHz to 100 mHz frequency range with 10 points per decade. At least three samples have been measured for each electrolyte composition for more consistent data. A detailed description of this method can be found in other papers.[17]

The charge–discharge half-cell cycling with graphite used the Li|electrolyte|graphite cell. A standard commercial single-coated graphite electrode from MTI-XTL was used in that experiment. The cut-off voltages were set to 0.1–2.6 V values. The current was chosen in such a way that both the discharge and charge processes would take 5 hours (C/5 rate). The half-cell contained 0.7 mol kg^{-1} LiTDPI in EC : DMC (1 : 2 weight ratio) as the electrolyte composition.

The charge–discharge half-cell cycling with LiNMO ($LiNi_{0.5}Mn_{1.5}O_4$) used the Li|electrolyte|graphite cell. A standard commercial LiNMO electrode from Sigma-Aldrich was used in that experiment. The cut-off voltages were set to 3.5–5.0 V values. The current was chosen in such a way that both the discharge and charge processes would take 5 hours (C/5 rate). The half-cell contained 0.7 mol kg^{-1} LiTDPI in EC : DMC (1 : 2 weight ratio) as the electrolyte composition.

2.2. Synthesis of lithium 5,6-dicyano-2-(trifluoromethyl) imidazopyrazine

The synthesis scheme is presented in Fig. 1.

16 g (0.1 mol) of 5,6-diamino-2,3-dicyanopyrazine (TCI Europe NV) was added to 350 ml of acetonitrile. Subsequently, 30.2 g (0.14 mol) of trifluoroacetic anhydride was added under an argon atmosphere to the reaction mixture and the mixture was then kept under reflux for 6 hours (reaction progress controlled by TLC). Upon vacuum evaporation to dry mass, the residue was dissolved in water, activated charcoal was added and they were stirred together for 10 minutes. The activated

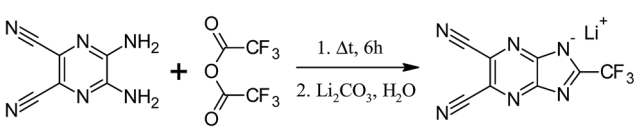

Fig. 1 Synthesis scheme for the lithium 5,6-dicyano-2-(trifluoromethyl)imidazopyrazine (LiTDPI) salt described in the text.

carbon was removed by filtering and the product was recrystallized from water. 19.6 g of 5,6-dicyano-2-(trifluoromethyl) imidazopyrazine was obtained (75% yield). T_m = 240–241 °C.

^{1}H NMR (DMSO-d_6): 11.75 (s, 1H, NH).

^{13}C NMR (DMSO-d_6): 157.65 (q, C–CF_3, J(C,F) = 39.2 Hz), 147.1 (s, 2C, C=C shared by both rings), 126.6 (s, 2C, C–CN), 119.1 (q, CF_3, J = 272.5 Hz), 115.2 (s, 2C, CN).

^{19}F NMR (DMSO-d_6): one peak (not calibrated).

9.8 g of 5,6-dicyano-2-(trifluoromethyl)imidazopyrazine was treated with 5.5 g of lithium carbonate (50% excess) suspension in water. The mixture was stirred for *ca.* 5 minutes. The precipitate was separated and the water solution was evaporated under vacuum to obtain the dry mass. The residue was dissolved in anhydrous acetonitrile and the undissolved precipitate was removed. The acetonitrile was evaporated under vacuum and the resulting salt was dried under vacuum at 110 °C for 24 hours. The lithium salt of 5,6-dicyano-2-(trifluoromethyl) imidazopyrazine was obtained as a result. The salt decomposes at 356 °C.

^{13}C NMR (DMSO-d_6): 164.8 (q, C–CF_3, J(C,F) = 35.7 Hz), 151.9 (s, 2C, C=C shared by both rings), 123.8 (s, 2C, C–CN), 120.8 (q, CF_3, J = 272.2 Hz), 116.1 (s, 2C, CN).

^{19}F NMR (DMSO-d_6): one peak (not calibrated).

3. Results and discussion

The thermal stability of the salt was tested by means of TGA (thermogravimetric analysis). The obtained results (Fig. 2) show a decomposition onset at 350 °C, which is a much higher temperature than for the most common salt in the battery industry, $LiPF_6$.[18] It is also much more stable than its benzimidazole analog, LiTDBI (272 °C). Unlike $LiPF_6$, and similarly to other imidazole-derived lithium salts, LiTDPI is stable in water solutions and is not susceptible to hydrolysis. This means easier handling and less restrictions for salt storage conditions. $LiPF_6$ on the other hand decomposes upon contact with trace moisture, not to mention forming solutions in it.[19]

The electrochemical stability of a salt is a key factor for electrolyte performance. LiTDPI was tested for its electrochemical stability by means of LSV. The LSV plot of 0.1 mol kg^{-1} LiTDPI solution in PC is presented in Fig. 3. The LiTDPI salt clearly shows stability up to 5.1 V *vs.* Li. This is more than enough for all kinds of contemporary electrode materials and allows for the application and use of the full potential of new electrode concepts.

The ionic conductivity of LiTDPI was tested first in PC—the model solvent for the organic carbonate family. Using a wide concentration range of the salt, within three orders of magnitude, allowed the impact of the association on conductivity to be seen as qualitative activation energy changes throughout the concentration range. On the other hand, the wide temperature range of measurements shows the stability of the new salt. Fig. 4 presents the results of the ionic conductivity measurements for the LiTDPI-PC solutions. The highest conductivity, 1.9 mS cm^{-1} at room temperature, was measured for the 0.5 mol kg^{-1} concentration. The conductivity at 0.2 mol kg^{-1} concentration is very similar and is equal to 1.8 mS cm^{-1}. The highest concentration, 1 mol kg^{-1}, which was also the maximum solubility of LiTDPI in PC, had a much smaller conductivity, 1.4 mS cm^{-1}. However, the activation energy for the highest concentration is clearly much higher than the activation energy for lower concentrations. Thus, the increase in the conductivity with temperature is much higher for high concentration solutions. So while at −20 °C, a solution of 1 mol kg^{-1} concentration starts from the same conductivity value as 0.1 mol kg^{-1}, at 60 °C it levels with the that of the 0.2 mol kg^{-1} solution, which is second to the 0.5 mol kg^{-1} ionic conductivity. Lower concentrations are ordered with their concentration in conductivity terms with the exception of the lowest one, 0.001 mol kg^{-1}, which has a conductivity of slightly higher than that of 0.002 mol kg^{-1} which might be the result of early association effects. Clearly, the different behavior of the 1 mol kg^{-1} concentration solution might be a result of it being the highest concentration, at the maximum solubility of LiTDPI in PC, with effects typically of higher viscosity and advanced association. The higher activation energy is the proof of such an argument.

Fig. 5 shows the behavior of LiTDPI solutions in an EC : DMC (1 : 2 weight ratio) mixture. It depicts an ionic conductivity *vs.* temperature plot. Due to the higher complexity of the system (ternary), association is more complicated, so it is

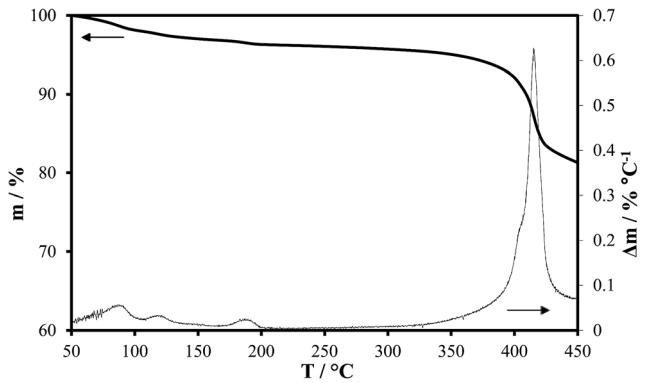

Fig. 2 Thermogravimetric analysis plot of the LiTDPI salt with the DTG plot.

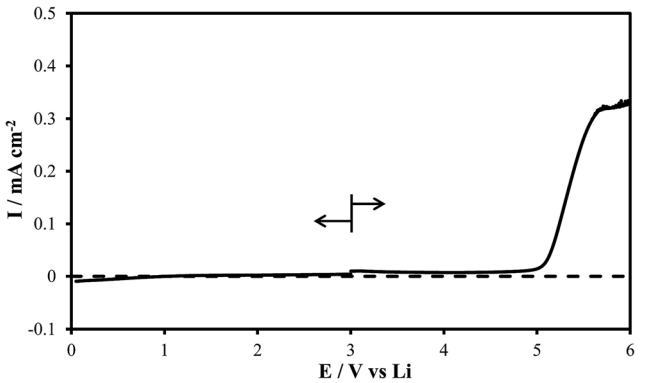

Fig. 3 Linear sweep voltammetry of the Li|0.1 mol kg^{-1} LiTDPI-PC|Pt system with lithium metal as the reference electrode.

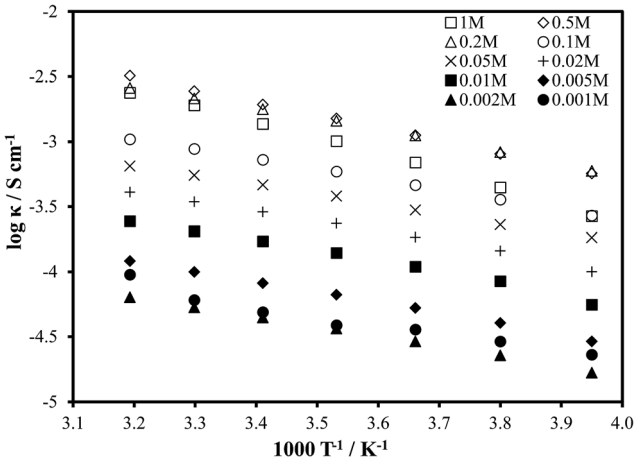

Fig. 4 Dependence of ionic conductivity on temperature for a wide range of LiTDPI concentrations in propylene carbonate.

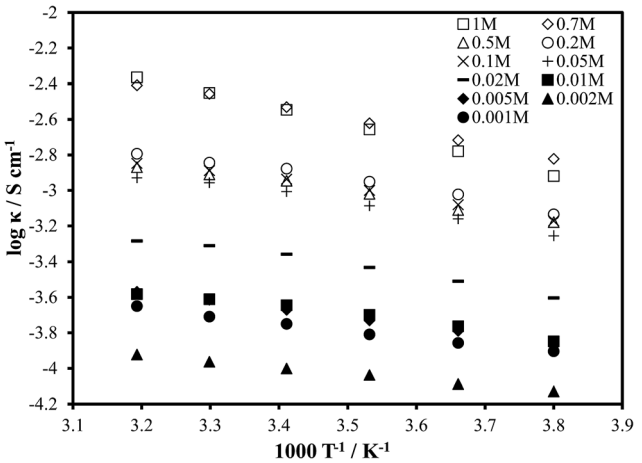

Fig. 5 Dependence of ionic conductivity on temperature for a wide range of LiTDPI concentrations in a mixture of ethylene carbonate and dimethyl carbonate (1 : 2 weight ratio).

not surprising that the conductivity dependence on concentration is more complicated than in the simpler system (LiTDPI-PC). Although at the lowest concentrations dependence is similar to the PC solutions, that is the conductivity of the 0.001 mol kg^{-1} solution is higher than that of the 0.002 mol kg^{-1} solution and the ionic conductivity of increasing concentrations from 0.002 mol kg^{-1} are monotonically rising. However, as soon as it is at 0.1 mol kg^{-1} it starts to change, because the 0.5 mol kg^{-1} conductivity (1.13 mS cm^{-1} at 20 °C) is lower than that of the 0.1 mol kg^{-1} (1.16 mS cm^{-1}). Above 0.5 mol kg^{-1} there is a sudden jump in the conductivity (2.94 mS cm^{-1}) at 0.7 mol kg^{-1} and a similar, but slightly smaller one, at 1 mol kg^{-1} (2.84 mS cm^{-1}). It is also plainly visible that the activation energies of the 0.7 and 1 mol kg^{-1} solutions are much higher than that of the lower concentration solutions. That last observation overlaps with the one made for the results of the PC solutions and strengthens the argument about the impact of association at such high concentrations.

Another very important parameter for electrolytes in order to assess their potential for real world application is the lithium cation transference number. It not only affects the yield of the charge–discharge cycle, but is also a factor in the lithium cation conductivity when multiplied by ionic conductivity. The lithium cation conductivity is a key factor for the evaluation of the electrolyte, as it also affects the rate capability of the final cell. In the case of LiTDPI, the solutions with concentrations which show high lithium cation transference number values overlaps with those of high ionic conductivity. In this, LiTDPI is similar to other weakly-coordinating imidazole-derived anions, but it is different from most other, mostly inorganic, cations. The latter usually has a reciprocal dependency between the lithium cation transference number and the ionic conductivity. Fig. 6 presents the results of the transference number measurements for the LiTDPI solutions in both PC and in a mixture of EC and DMC (1 : 2 weight ratio). The results for the PC solutions are slightly better on average than the ones for the EC : DMC mixture, they are also more stable throughout the concentration range with a notable exception of the highest concentration (1 mol kg^{-1}). Even though the lithium cation transference numbers of the EC : DMC solutions have decreased values for the 0.001–0.01 mol kg^{-1} range, the most important results from an application point of view are relatively high and surpass the 0.4 value. It is also important that a high lithium cation transference number overlaps with the highest conductivity, yielding lithium cation conductivity of over 1 mS cm^{-1} (*e.g.* at 1 mol kg^{-1}, 2.84 mS cm^{-1} × 0.43 = 1.22 mS cm^{-1}). There is also a very high value of the lithium cation transference number for the 1 mol kg^{-1} solution of LiTDPI in PC, namely 0.55, which is much higher than traditional, inorganic lithium salts.

Finally, for the final proof that it is possible to apply the LiTDPI salt as a lithium conducting electrolyte and that it has potential for application in energy storage, preliminary half-cell cycling experiments were performed. A graphite|0.7 mol kg^{-1} LiTDPI-EC : DMC (1 : 2)|Li half-cell was assembled and tested with charge–discharge cycling. Fig. 7 shows the result of such

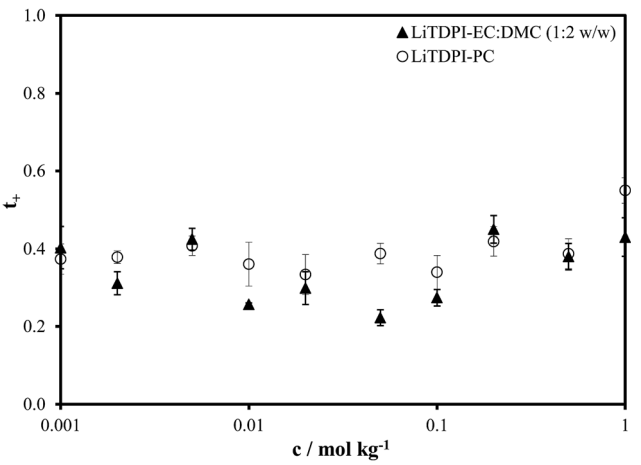

Fig. 6 Dependence of the lithium cation transference number on the LiTDPI concentration in propylene carbonate and in a mixture of ethylene carbonate and dimethyl carbonate (1 : 2 weight ratio).

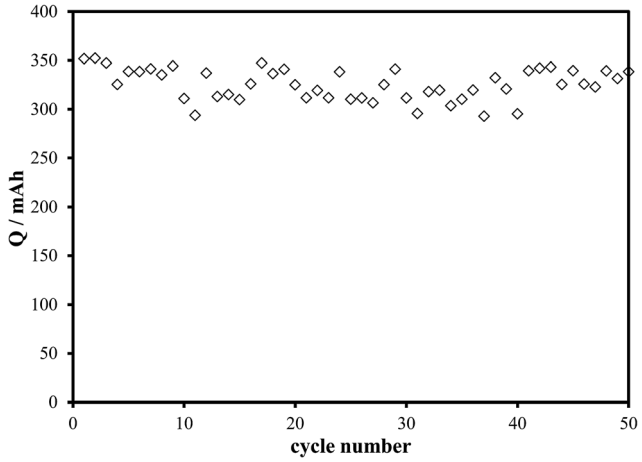

Fig. 7 Discharge anodic capacities during cycling of the graphite|0.7 mol kg^{-1} LiTDPI-EC : DMC (1 : 2 weight ratio)|Li half-cell at the C/5 rate.

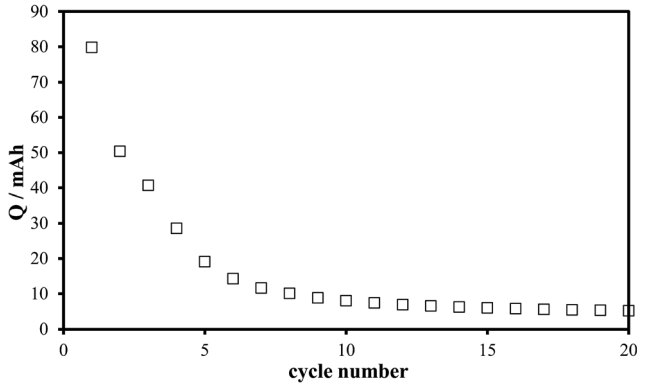

Fig. 9 Discharge cathodic capacities during cycling of the LiNMO ($LiNi_{0.5}Mn_{1.5}O_4$)|0.7 LiTDPI-EC : DMC (1 : 2 weight ratio)|Li half-cell at the C/5 rate.

cycling. It begins at quite a high capacity of 351 mA h g^{-1}, while the theoretical value for the capacity of graphite is 372 mA h g^{-1}. Thus, it is 94% of the theoretical value. Moreover, after 50 cycles the capacity retention is very good, as it keeps on a similar level until the 50^{th} cycle, at which point it is 338 mA h g^{-1}, so it is 96% of the initial capacity. That proves that LiTDPI is compatible with the graphite anode and that it is very stable as an electrolyte. Also, it is not decomposing at the high or low voltages applied to the cell during cycling.

Two additional preliminary measurements were made for the purpose of testing the potential of LiTDPI to use in high-voltage cells. Firstly, the corrosiveness of 0.7 mol kg^{-1} LiTDPI in EC : DMC (1 : 2 weight ratio) against an aluminum collector was tested. The result of this measurement is shown in Fig. 8. Even though the CV rate was very slow (0.1 mV s^{-1}), there is no visible sign of corrosion until 4.6 V *vs.* Li and even then it is not abrupt (until 5.1 V *vs.* Li). Secondly, the same 0.7 mol kg^{-1} LiTDPI in EC : DMC (1 : 2 weight ratio) electrolyte was preliminarily tested with the high-voltage cathode in the $LiNi_{0.5}Mn_{1.5}O_4$|0.7 mol kg^{-1} LiTDPI-EC : DMC (1 : 2)|Li half-cell. The result of the cycling is shown in Fig. 9. Although the initial discharge capacity is quite good (80 mA h g^{-1}), it is decreasing steadily and fast. As the electrolyte was not optimized for these measurements and it is the only cathode material tested so far, it is possible that LiTDPI is not compatible with this particular cathode. Also, the formation of the cell should be optimized, which was not the case here. However, even that very preliminary test proves the salt stability against high potentials in the cell, which was the main reason for this measurement.

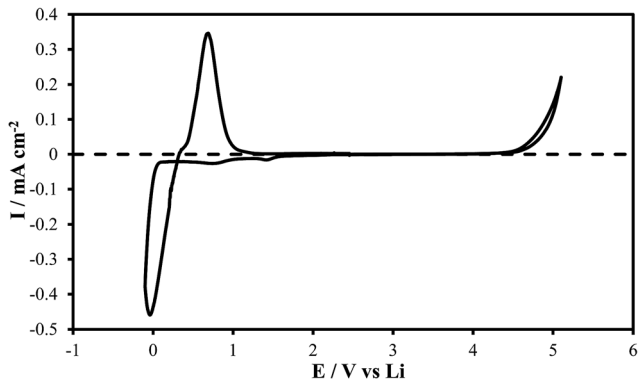

Fig. 8 Cycling voltammetry of the Li|0.7 mol kg^{-1} LiTDPI-PC|Al system with lithium metal as the reference electrode.

The results obtained for the LiTDPI solutions are very important, because they show that it is possible to tweak the structure of the anion of the salt in a way so that no property is getting worse and no parameter is getting lower. Although the difference between the TDPI and TDBI anions (benzimidazole *vs.* imidazopyrazine rings) is not very big, neither it is subtle. The change proposed here improves most of the parameters distinctively and consistently. Improvement takes place for both thermal and electrochemical stability (by almost 80 °C and 0.35 V, respectively). This means that the ring has a higher stability due to the HOMO energy level change as a result of the structural change. Also, the ionic conductivity and lithium cation conductivity are better, which can be explained by a weaker coordination of the lithium cation and higher mobility of the anion. The weaker coordination and higher mobility are affecting the transference numbers and association leads to the lithium cation conductivity. The weaker coordination, lower association level and stability improvement are the results of getting rid of the hydrogen atoms. Hydrogen atoms are prone to forming hydrogen bonds with the solvent (especially solvents such as carbonates) and will be the weakest link in terms of stability (radical formation). The other beneficial properties of the structures are left, meaning symmetry, the presence of electron withdrawing groups and the aromatic skeleton (so-called Hückel anions). Thus, the main reasoning of the concept has been proven, that the assumed improvement of the structure is in fact the improvement of practical features.

4. Conclusions

In the present work, we have presented the synthesis, characteristics and basic properties of the solutions of a completely

new lithium salt tailored for application as a lithium-ion conducting electrolyte. The aim was to obtain a new weakly-coordinating anion that could provide better ionic transport than previous generations of lithium salts, while keeping good safety and ease of handling properties. The synthesis of the anion itself is a one-step reaction and is easy in terms of handling the substrates and the product, as no special means, equipment or material purity are needed for an effective synthesis. We also characterized this new substance with basic spectral data and studied its thermal and electrochemical stabilities, which are very good compared to the state-of-the-art salt ($LiPF_6$), namely up to 350 °C and 5.1 V *vs.* Li. Thus, it is much more stable than its other imidazole-derived predecessors, like LiTDI or an even newer one, LiTDBI (another salt with a two-ring aromatic anion). Basic tests also show good transport properties, with a two-fold increase in conductivity compared to LiTDBI, close to 3 mS cm^{-1}, and a similar lithium cation transference number, over 0.4. Overall, the lithium cation conductivity (ionic conductivity multiplied by the lithium cation transference number), as well as the safety/stability of the new LiTDPI salt is better than LiTDBI, which is undoubtedly an advance. It is also proof of the possible achievements from using Hückel-type weakly-coordinating anions. Finally, as a proof of concept, an electrolyte containing LiTDPI was preliminary tested in a half-cell with a graphite anode, showing good compatibility and excellent capability retention over 50 cycles. There is also no difference in the good performance with the electrode compared to LiTDBI, which is another success of the new anion. All of these LiTDPI benefits and the lack of negative differences towards LiTDBI confirm the initial assumption that removing the hydrogens from the anion structure would be beneficial for the salt performance. Apart from achieving theoretical objectives, LiTDPI is also proving, with its great half-cell performance, that there is application potential for that salt and that it deserves more interest in the future.

Acknowledgements

This work was financially supported by Warsaw University of Technology. The research leading to these results has received funding from the European Union Seventh Framework Programme (FP7/2007-2013) under grant agreement number 608502 (Project SIRBATT).

References

1 Lux Research, Beyond Lithium-Ion: A Roadmap for Next-Generation Batteries, March 2013, LREVI-R-13–1.
2 M. Marcinek, J. Syzdek, M. Marczewski, M. Piszcz, L. Niedzicki, M. Kalita, A. Plewa-Marczewska, A. Bitner, P. Wieczorek, T. Trzeciak, M. Kasprzyk, P. Łężak, Z. Zukowska, A. Zalewska and W. Wieczorek, *Solid State Ionics*, 2015, **276**, 107.
3 T. Kawamura, S. Okada and J.-I. Yamaki, *J. Power Sources*, 2006, **156**, 547.
4 H.-B. Han, S.-S. Zhou, D.-J. Zhang, S.-W. Feng, L.-F. Li, K. Liu, W.-F. Feng, J. Nie, H. Li, X.-J. Huang, M. Armand and Z.-B. Zhou, *J. Power Sources*, 2011, **196**, 3623.
5 X. Zhang, P. N. Ross Jr, R. Kostecki, F. Kong, S. Sloop, J. B. Kerr, K. Striebel, E. J. Cairns and F. McLarnon, *J. Electrochem. Soc.*, 2001, **148**, A463.
6 R. Jasinski and S. Carroll, *J. Electrochem. Soc.*, 1970, **117**, 218.
7 A. Webber, *J. Electrochem. Soc.*, 1991, **138**, 2586.
8 S.-T. Myung, M. Hitoshi and Y.-K. Sun, *J. Mater. Chem.*, 2011, **21**, 9891.
9 K. Xu, S. Zhang and T. R. Jow, *Electrochem. Solid-State Lett.*, 2005, **8**, A365.
10 L. Niedzicki, G. Z. Żukowska, M. Bukowska, P. Szczeciński, S. Grugeon, S. Laruelle, M. Armand, S. Panero, B. Scrosati, M. Marcinek and W. Wieczorek, *Electrochim. Acta*, 2010, **55**, 1450.
11 L. Niedzicki, S. Grugeon, S. Laruelle, P. Judeinstein, M. Bukowska, J. Prejzner, P. Szczeciński, W. Wieczorek and M. Armand, *J. Power Sources*, 2011, **196**, 8696.
12 D. W. McOwen, *Developing New Electrolytes for Advanced Li-ion Batteries*, Ph.D. thesis, North Carolina State University, Raleigh, North Carolina, 2014.
13 L. Niedzicki, P. Oledzki, A. Bitner, M. Bukowska and P. Szczecinski, unpublished work.
14 J. Scheers, P. Johansson, P. Szczecinski, W. Wieczorek, M. Armand and P. Jacobsson, *J. Power Sources*, 2010, **195**, 6081.
15 *Handbook of Batteries*, ed. D. Linden and T. B. Reddy, McGraw-Hill, 3rd Edition, 2002.
16 P. G. Bruce and C. A. Vincent, *J. Electroanal. Chem.*, 1987, **225**, 1.
17 L. Niedzicki, M. Kasprzyk, K. Kuziak, G. Z. Zukowska, M. Marcinek, W. Wieczorek and M. Armand, *J. Power Sources*, 2011, **196**, 1386.
18 X.-G. Teng, F.-Q. Li, P.-H. Ma, Q.-D. Ren and S.-Y. Li, *Thermochim. Acta*, 2005, **436**, 30.
19 A. V. Plakhotnyk, L. Ernst and R. Schmutzler, *J. Fluorine Chem.*, 2005, **126**, 27.

